Earthquakes and Structures, *Vol. 17, No. 4* (*2019*) *387-398*
DOI: https://doi.org/10.12989/eas.2019.17.4.387

The critical angle of seismic incidence of transmission tower -line system based on wavelet energy method

Li Tian[1a], Xu Dong[1b], Haiyang Pan[*1] and Xiaoyu He[2c]

[1]*School of Civil Engineering, Shandong University, Jinan, Shandong Province 250061, China*
[2]*Zhejiang Provincial Institute of Communication Planning, Design and Research, Hangzhou, Zhejiang Province 310006, China*

(*Received July 21, 2019, Revised September 3, 2019, Accepted September 4, 2019*)

Abstract. On the basis that ground motions may arrive at a structure from any horizontal direction and that different directions of seismic incidence would result in different structural dynamic responses, this paper focuses on orienting the crucial seismic incidence of transmission tower-line systems based on the wavelet energy method. A typical transmission tower-line system is chosen as the case study, and two finite element (FE) models are established in ABAQUS, with and without consideration of the interaction between the transmission towers and the transmission lines. The mode combination frequency is defined by considering the influence of the higher-order modes of the structure. Subsequently, wavelet transformation is performed to obtain the total effective energy input and the effective energy input rate corresponding to the mode combination frequency to further judge the critical angle of seismic incidence by comparing these two performance indexes under different seismic incidence angles. To validate this approach, finite element history analysis (FEHA) is imposed on both FE models to generate comparative data, and good agreement is found. The results demonstrate that the wavelet energy method can forecast the critical angle of seismic incidence of a transmission tower-line system with adequate accuracy, avoiding time-consuming and cumbersome computer analysis. The proposed approach can be used in future seismic design of transmission tower-line systems.

Keywords: critical incidence angle; transmission tower-line system; wavelet transformation; effective energy input; effective energy input rate

1. Introduction

Of existing structures, electricity transmission systems have been widely recognized as lifeline systems, which undertake the important task of transporting and distributing the electrical power from power plants to customers. Due to the strong dependencies of modern life on electrical power, transmission tower-line systems will inevitably be constructed in the regions with various extreme conditions, especially high intensity. This implies that transmission tower-line system should possess an extraordinary capacity to resist seismic shock. Nevertheless, historically, transmission towers have failed and even collapsed during major earthquakes, such as the 1994 Northridge earthquake (Hall *et al*. 1994), the 1995 Kobe earthquake (Shinozuka 1995), the 1999 Chi-Chi earthquake (Zhang *et al*. 2012) and the 2008 Wenchuan earthquake (Zhao *et al*. 1994). Additionally, the failure of transmission towers may trigger the failure of the entire power grid via a domino effect, directly leading to not only tremendous economic losses but also a long-duration blackout. Following the above premises, it is imperative to clearly investigate seismic responses and evaluate the structural seismic performance of the transmission towers exposed to earthquakes.

In recent decades, many research efforts have been dedicated to investigating the seismic responses of transmission tower-line systems. Ghobarah *et al*. (1996) investigated the effect of multi-support excitations on the lateral seismic responses of overhead power transmission lines. Li *et al*. (2005) proposed a simplified method to investigate the out-of-plane and in-plane vibrations of a transmission tower-line system subjected to seismic excitations. Lei and Chien (2009) investigated the structural dynamic response of transmission towers linked together through transmission lines and obtained better insight into the interaction between towers and wires. Notably, all the aforementioned analyses have concerned the seismic responses of transmission tower-line systems subjected to far-field ground motions. However, compared to far-field ground motions, near-fault ground motions can result in more serious structural dynamic responses due to the intense velocity and long period of the displacement pulses; consequently, such motions have recently attracted widespread interest from researchers and engineers. Wu *et al*. (2014) investigated the seismic response of a large crossing transmission tower-line (LCTL) system subjected to near-fault ground motions, and the results showed that the seismic responses increase with the pulse period of the near-fault ground motions. Tian *et al*. (2019a) performed the fragility analysis of transmission tower-line systems

∗Corresponding author, Ph.D.
E-mail: phy930504@163.com
[a]Professor
[b]M.D. Student
[c]Associate Professor

ISSN: 2092-7614 (Print), 2092-7622 (Online)

subjected to near-fault ground motions and demonstrated the effects of near-fault ground motions on the seismic response of such systems. These results of the above studies imply that the effects of near-fault ground motions cannot be ignored in structural design. However, the ultimate capacity (i.e., collapse) of a transmission tower-line system was not studied in the above analyses. Subsequently, seismic-induced collapse analysis was conducted. Albermani *et al*. (2003, 2009) developed a nonlinear analytical technique to simulate the collapse of transmission towers, which was confirmed by comparison with full-scale test results. Eslamlou and Asgarian (2017) performed a nonlinear dynamical analysis for modeling the progressive collapse of a transmission tower and evaluated the critical elements and sensitive areas of the structure. Tian *et al*. (2017, 2019c) and Zheng *et al*. (2017) simulated the progressive collapse of transmission towers during earthquakes by considering the buckling and post-buckling behaviors of the members, respectively.

The directions of ground motion input were generally applied along the fixed reference axis of the transmission tower-line system in all the aforementioned analyses. However, in practice, the ground motions are not perfectly aligned in a particular direction. Ignoring the uncertainty in the seismic incidence angle will cause the structural dynamic response to be underestimated, resulting in an inaccurate performance evaluation. Moreover, the significant influence of incidence angle on structural seismic response has been verified in different conventional structures, such as reinforced concrete (RC) frames (Magliulo *et al*. 2014, Cantagallo *et al*. 2012), bridges (Roy *et al*. 2018, Torbol *et al*. 2012), transmission tower-line systems (Tian *et al*. 2018, 2019a) and other structures (Huang *et al*. 2016, Rigato *et al*. 2007). Considering these facts, researchers have worked to develop an effective approach to determine the critical angle of ground motion incidence of structures. Wilson and Button (1982) developed a simple method to evaluate the critical angle of ground motion incidence corresponding to the maximum displacements but without considering any correlation between the horizontal ground motion components. Based on the random vibration theory, Smeby and Der Kiureghian (1985) proposed an explicit approach using random vibration theory to determine the critical angle of asymmetric buildings by considering the proper correlation between two horizontal ground components. In addition, many methods have also been deployed to determine the critical incidence angle and the corresponding maximum response based on different rules and theories, such as the square root sum of squares (SRSS) (Lopez *et al*. 2000), complete quadratic combination (CQC) (Lopez *et al*. 1997, Menun and Der Kiureghian 1998), the extended Penzien-Watabe medel (Fujita and Takewaki 2010) and response spectrum (Feng and Li 1991). However, it is unclear if the method can be suited for the transmission tower-line systems, because the transmission tower-line systems are significantly different from those structures considered in previous works. Therefore, there is a need to develop a reliable and practical method for determining the critical angle of seismic incidence of transmission tower-line systems.

Wavelet transform is a new transform analysis method developed from the basic idea of short-time Fourier transform localization analysis; this method overcomes the shortcomings of other methods, for which the window size cannot change with frequency. As an ideal analysis tool, the wavelet analysis method has been widely utilized in recent years but has mostly been used for structural health monitoring (Taha *et al*. 2006, Bravo-Imaz *et al*. 2017, Wimarshana *et al*. 2017) and damage identification (Kim and Melhem 2004, Bombale *et al*. 2008, Montanari *et al*. 2015) of structures. Additionally, few studies regarding the application of this method to transmission tower-line systems were found, especially for determining the critical incidence angle.

The objective of this investigation is to provide an efficient and convenient method for determining the critical angle of seismic incidence of transmission tower-line systems. Considering the merits of wavelet transform, the wavelet energy method by combining the energy input of a ground motion and the natural frequency of a structure is present in this study. To take the higher-mode effect into account, the mode combination frequency is developed by the square root of sum of squares (SRSS) rule. To validate this approach, two FE models (including transmission single tower and transmission tower-line system) are constructed in ABAQUS, and the corresponding finite element history analysis (FEHA) is imposed. The resulting database from the FEHA is subsequently used to evaluate the adequacy of the wavelet energy method. The rest of this paper is organized as follows: Section 2 describes the prototype structure of a transmission tower-line system and develops its FE model in ABAQUS software; the wavelet energy method and the application process for orienting the critical seismic incidence are introduced in Section 3; in Section 4, a suite of eight ground motion records are selected for the wavelet analysis and time history analysis; FEHA is performed, and the numerical results are compared with those from the wavelet energy method in Section 5. Finally, Section 6 synthesizes the major conclusions of this research.

2. Prototype structure and FE model

A typical actual 500 kV transmission tower-line system prototype, located in Northeast China, is chosen as a background project in the present study. The transmission tower is categorized as SZ12 according to the Rules of Nomenclature for Transmission Poles and Towers (GB 2695-82, 1982), and most of this transmission line is located in the 8-degree seismic design zone specified in the Seismic Ground Motion Parameters Zonation Map of China (GB 18306-2015, 2015). Based on the Code for Seismic Design of Electrical Installations (GB 50260-2013, 2013), the region where the transmission tower-line system located is defined as the type of site conditions II, and the tower is designed for the seismic hazard with the peak ground acceleration (PGA) of 0.2 g, which corresponds to the exceeding probability of 10% in 50 years This prototype

Table 1 Specifications and performance indexes of the conductors and ground wires

Type	Conductors	Ground wires
Transmission line type	LGJ-400/35	LGJ-95/55
Outer diameter (m)	26.82E-3	16.00E-3
Cross-sectional area (m^2)	425.24E-6	152.81E-6
Elastic modulus (GPa)	65.00	105.00
Mass per unit length (kg/m)	1.3490	0.6967
Coefficient of linear expansion (1/°C)	2.05E-5	1.55E-5

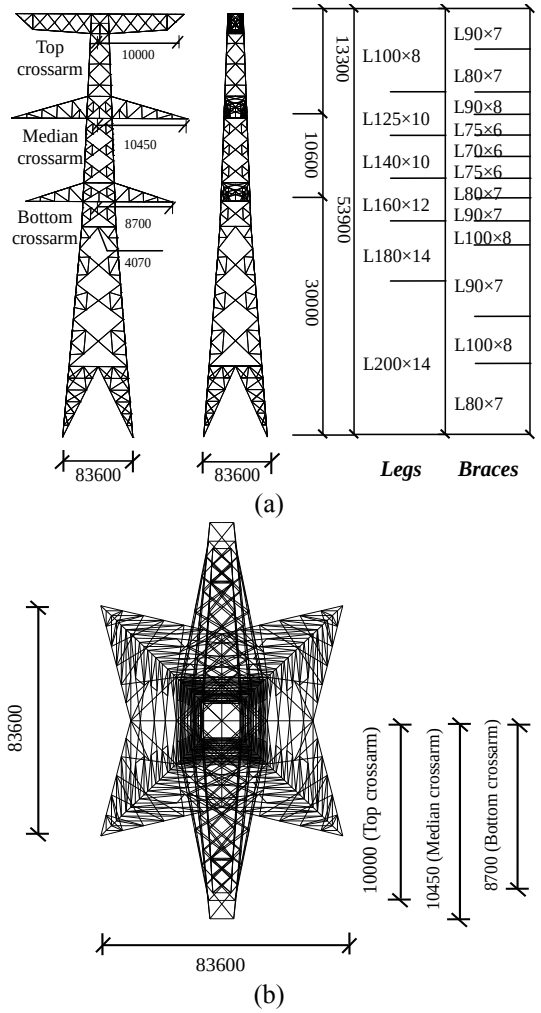

Fig. 1 Configuration of the transmission tower: (a) elevation; (b) plan (unit: mm)

structure is selected due to the following causes: (1) There is detailed design information available for the system; (2) the system is located in a seismic region; and (3) the system has been studied in a previous paper (Tian *et al*. 2019b). The transmission tower-line system consists of three transmission towers with the same design and four transmission lines with the equal span of 400 m. This supporting tower is designed based on the Code for Design of 110 kV–750 kV Overhead Transmission Line (GB 50545-2010, 2010), and the geometry and cross-section of the transmission tower are illustrated in the Fig. 1. As shown, the transmission tower is constructed with a total height of 53.9 m, a square base of 8.36 m×8.36 m and a self-weight of 20.23 tonnes, primarily consisting of a tower body and three cross arms (the Top, Median and Bottom cross arms). The leg members are fabricated by Q345 angle steel, whereas the diagonal members are made of Q235 angle steel. Regarding the transmission lines, the conductor lines are JL1/LHA1-465/210 supported at the Top, Median and Bottom cross arms, while the ground wires are OPGW-185 hanging at the Top cross arms. Table 1 summarizes the parameters of the conductors and ground wires in detail.

Table 2 Summary of structural period and participating mass factors

FE model	Modal order	Longitudinal direction (X direction)		
		Period (s)	Frequency (Hz)	Participating mass factor
Model I	1	0.56	1.78	0.49
	2	0.20	5.00	0.22
	3	0.18	5.56	0.13
Model II	1	0.73	1.37	0.28
	2	0.63	1.59	0.15
	3	0.21	4.76	0.15

The detailed FE model of the prototype structure is built using ABAQUS (version 6.12), which is a professional commercial software that can be used for simulating structural seismic response. Two models, including single-tower and tower-line system models (denoted Models I and II, respectively), are developed. Fig. 2 describes both Models I and II. The members of the transmission tower are modeled by using beam elements (B31) in both models, and the mechanical properties of the members are assigned to have an elastic modulus of 201 GPa, yield stress of 235 MPa for Q235 (345 MPa for Q345), mass density of 7850 kg/m^3 and Poisson's ratio of 0.3. Notably, there are a total of 1716 elements and 677 nodes in the developed model transmission tower. To simplify the analysis, it is assumed that the bottom of the transmission tower is fixed on the ground, without considering soil-structure interactions. Additionally, the truss elements (T3D2) were used for the transmission lines. Each transmission line is divided into 100 elements, and the materials of the lines are assumed to be under tension only. The outermost ends of each side-span transmission line are hinged at the same height on the adjacent transmission towers. Note that all the seismic response analyses are performed in the elastic stage. The damping ratios of the transmission tower and lines are assumed to be 2% and 1%, respectively. Furthermore, eigenvalue analysis is performed to obtain the structural natural vibration periods and corresponding participating mass factors, and the analysis results are summarized in Table 2.

3. Wavelet energy method

Compared to traditional Fourier transforms, wavelet transforms can not only realize the simultaneous analysis and processing of the seismic wave in the time-frequency domain, but also decompose the ground motion energy

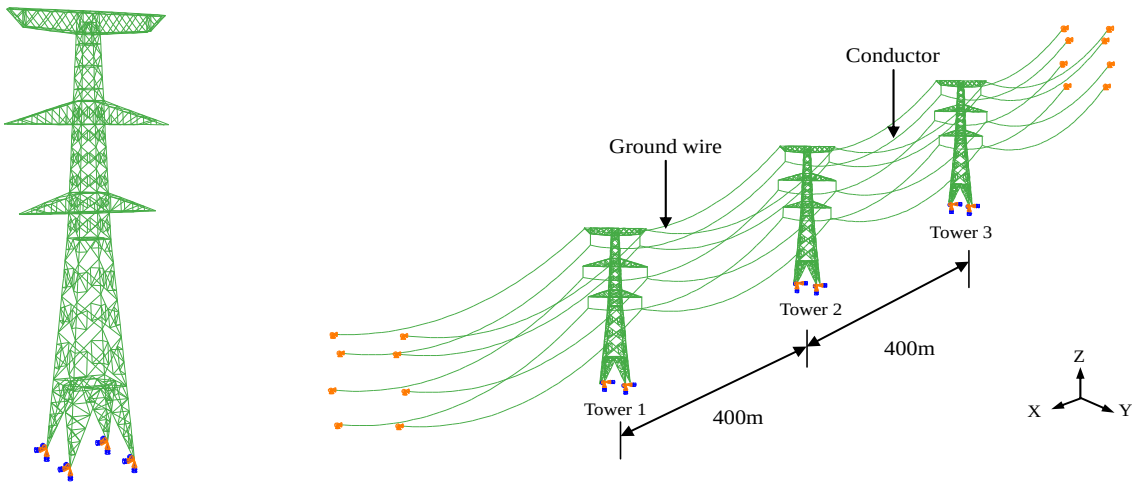

(a) (b)

Fig. 2 FE model: (a) transmission single tower; (b) transmission tower-line system

input into the energy of different frequency components. Therefore, the wavelet energy method is employed to predict the critical angle of seismic incidence of the transmission tower-line system in this section. Here, the principle and application of the wavelet energy method are briefly introduced, and concerned readers can find more information in a previous study (Li *et al.* 2009).

3.1 Effective energy input of ground motion

Previous studies (Uang and Bertero 1990, Fajfar and Vidic 1994, Taniguchi *et al.* 2016 Akehashi and Takewaki 2019) have demonstrated that the total energy input of the ground motion (the total amount of energy during the ground motion) has a significant impact on the dynamic analysis of a structure. Note that the total energy input is equivalent to the acceleration power, E, of the ground motion, thus, the total energy input could be calculated by integrating the original acceleration information, $a_g(t)$, over the whole duration, as follows (Li *et al.* 2009)

$$E^k = \int_0^{(k-1)\Delta t} \left| a_g(t) \right|^2 dt = \sum_{i=1}^{n-1} E_i^k \tag{1}$$

$$E_i^k = c_\psi^{-1} \frac{\Delta b}{2} \frac{\Delta a}{2} \left[e_i^1 + e_i^k + e_{i+1}^1 + 2\sum_{j=2}^{k-1} \left(e_i^j + e_{i+1}^j \right) \right] \tag{2}$$

where, the superscript k is a time-variable representing the moment, $(k-1)\Delta t$. For an acceleration record with m data points, E^m represents the total energy input of the ground motion, and the subscript i is a frequency-dependent variable that represents the frequency component of the ground motion.

For a seismic record, although the total energy input of the ground motion remains constant, it may result in different dynamic responses for different structures. This is because the seismic record contains various energy components with different frequencies (see Eq. (1)), and selective absorption and amplification effects on the energy of different frequency components are caused when total energy is input into structures. Additionally, the dynamic response of a structure can be most affected by the energy of the frequency component equal to the particular natural frequency (generally fundamental frequency) of the structure, which is herein defined as effective energy input, E_p^m.

3.2 Effective energy input rate

Notably, different ground motions with identical effective energy inputs can also cause distinct dynamic responses for the same structures (Kuwamura *et al.* 2017a, Kuwamura *et al.* 2017b). This indicates that the dynamic behavior of a structure during an earthquake is a complicated nonstationary process not only in the frequency domain but also in the time domain. Therefore, equally as important as the effective energy input, the effective energy input rate has a significant influence on the dynamic response of a structure during an earthquake (Takewaki *et al.* 2013, Yamamoto *et al.* 2011). The input rate of effective energy is defined as follows

$$RE_p^k = (E_P^{k+N} - E_P^k) / (N \cdot \Delta t) \tag{3}$$

$$N = T / (2 \cdot \Delta t) \tag{4}$$

where, RE_p^k represents the instantaneous input rate corresponding to the time, $(k-1)\Delta t$. T is the natural period of the structure.

In previous research (Li *et al.* 2009), T is regarded as equal to the fundamental period t of the structure. However, to consider the influence of higher-order modes, the square root of sum of squares (SRSS) rule, originally proposed by Rosenblueth (1951), is adopted to obtain the period for the combination of modal contributions in this paper. The corresponding mode period $\bar{T}$ and frequency $\bar{\mathrm{f}}$ can be respectively calculated as follows

$$\bar{T} = \sqrt{\sum_1^n \left[T_n \left(\frac{\Gamma_n}{\Gamma_1} \right) \right]^2} \tag{5}$$

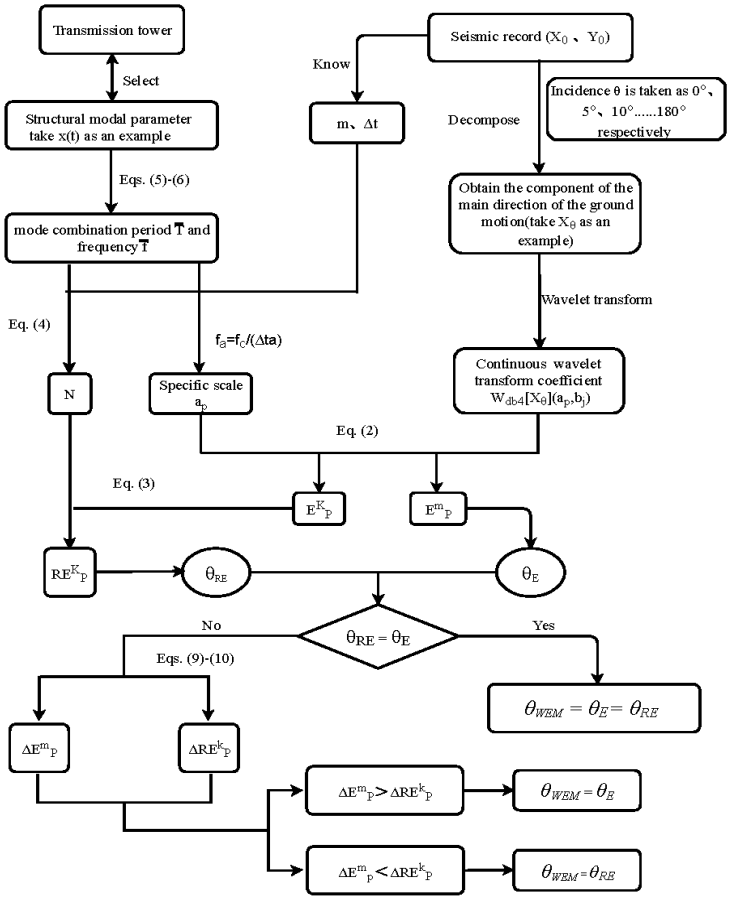

Fig. 3 The flow chart for the determination of earthquake critical incidence angle of a transmission tower-line system

$$\bar{f} = 1/\bar{T} \tag{6}$$

where T_n represents the period of the nth mode and Γ_n represents the participating mass factor of the n_{th} mode.

3.3 Steps to determine earthquake critical incidence angle

The flow chart for the forecast of the most unfavorable ground motion incidence angle of the transmission tower-line system based on the presented wavelet energy method is plotted in Fig. 3.

The seismic records with two horizontal components (the vertical component may be included, if needed) should be addressed using the orthogonal decomposition method to obtain two new horizontal components with different input angles. As illustrated in Fig. 4, it is assumed that θ is an angle between the X direction (the longitudinal direction of the transmission tower) and X_0 direction, and the clockwise direction is a positive direction. Specifically, the case in which the seismic component X_0 is input along the X direction and the seismic component Y_0 is input along the Y direction (the lateral direction of the transmission tower) is defined as the incidence angle of 0°. X_0 and Y_0 represent the two horizontal components of the ground motion, while the two new horizontal components with different input angles θ are symbolized as X_θ and Y_θ, respectively. Additionally, $\ddot{u}_{x_o}(t)$ and $\ddot{u}_{y_o}(t)$ denote the acceleration time histories

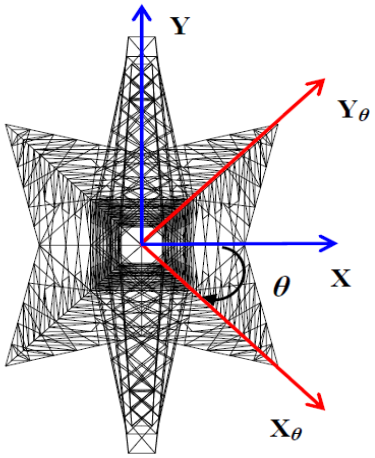

Fig. 4 Definition of incidence angle

recorded along the X_0 and Y_0 directions, respectively. When the seismic record acts on the transmission tower-line system with different incidence angles, the new acceleration time histories of two horizontal components $\ddot{u}_X(\theta, t)$ and $\ddot{u}_Y(\theta, t)$ can be obtained by decomposing the acceleration time histories $\ddot{u}_{x_o}(t)$ and $\ddot{u}_{y_o}(t)$ as follows

$$\ddot{u}_X(\theta, t) = \ddot{u}_{x_o}(t)\cos(\theta) + \ddot{u}_{y_o}(t)\sin(\theta) \tag{7}$$

$$\ddot{u}_Y(\theta, t) = -\ddot{u}_{x_o}(t)\sin(\theta) + \ddot{u}_{y_o}(t)\cos(\theta) \tag{8}$$

Table 3 Selected ground motion records

ID	Earthquake	Site classification	Magnitude	Station, Component	PGA/g
GM1	Langcang	I	6.7	Zhutang A S00E/S90E	0.553/0.529
GM2	Michoacan Mexico	I	8.1	La Union N90E/N00E	0.150/0.166
GM3	Imperial Valley	II	6.9	El Centro Array#10 N69W/N21E	0.172/0.226
GM4	Gengma1	II	4.1	Gengma S00E/S90E	0.143/0.137
GM5	Gengma2	III	4.6	Gengma S00E/S90E	0.092/0.094
GM6	Morgan Hill	III	6.2	Coyote Lake Dam CA285/ CA195	0.653/1.162
GM7	Tangshan	IV	6.9	Tianjin Hospital WE/SN	0.106/0.149
GM8	Westmoreland	IV	5.6	Westmoreland 0/90	0.444/0.361

Since both the single transmission tower and transmission tower-line system are symmetrical in both the X and Y directions (see Fig. 4), the incidence angle ranges from 0° to 180°. Interested readers can find more information about the incidence angle varying from 180° to 360° for the asymmetric structures in the study (Tian *et al.* 2018).

After obtaining the mode combination period, the wavelet transform tool in MATLAB is used to perform a continuous wavelet transform on the seismic wave components X_θ and Y_θ, to calculate the time series of the total effective energy input of the seismic wave, E_p^m and the effective energy input rate, RE_p^k. Note that the selection of the mother wavelet function may influence the accuracy of the wavelet transform, and it is complicated to conduct the corresponding research on all the existing wavelet functions. Therefore, the Daubechies wavelet with N=4 (denoted as Db4) is applied as the mother wavelet function in the present study; this wavelet can provide an adequate balance between the time domain and frequency domain (Baranov 2007), and the center frequency of the wavelet is 0.71 Hz.

Notably, with respect to E_p^m and RE_p^k, the incident angle candidates, θ_E and θ_{RE}, can be considered the critical incident angle. Therein, θ_E is selected when E_p^m obtains the maximum value, while θ_{RE} is chosen when E_p^m reaches the maximum value. If θ_E is equal to θ_{RE}, either can be defined as the critical incident angle; If not, the parameters ΔE_p^m and ΔRE_p^k must be calculated, and the critical incident angle is eventually approved by comparing the two parameters. ΔE_p^m and ΔRE_p^k can be obtained by the following expressions

$$\Delta E_p^{\mathrm{m}} = \frac{E_p^{\mathrm{m}}(\theta_E) - E_p^{\mathrm{m}}(\theta_{RE})}{E_p^{\mathrm{m}}(\theta_E)} \times 100\% \tag{9}$$

$$\Delta RE_p^k = \frac{\max\left[RE_p^k(\theta_{RE})\right] - \max\left[RE_p^k(\theta_E)\right]}{\max\left[RE_p^k(\theta_{RE})\right]} \times 100\% \tag{10}$$

4. Selection of seismic waves

In this paper, a family of 8 ground motion records are selected based on a previous study (Xie and Zhai 2003), and the detailed acceleration information of each seismic record is obtained from the database of the Pacific Earthquake Engineering Research Center (PEER, http://peer.berkeley.edu/). Note that these eight seismic records belong to four different types of site conditions I, II, III and IV. Table 3 summarizes the information of the 8 seismic records, including the year and name of each earthquake event, the magnitude and the site classification. These 8 records are taken from 7 events that occurred between 1976 and 1988 in four different countries. The corresponding event magnitudes range from 4.1 to 8.1, with an average magnitude of 6.1. Interested readers can find more information about the seismic records in the study (Xie and Zhai 2003). Fig. 5 shows the acceleration spectra of the selected ground motions (gray thin lines) and the corresponding mean spectrum (blue thick line).

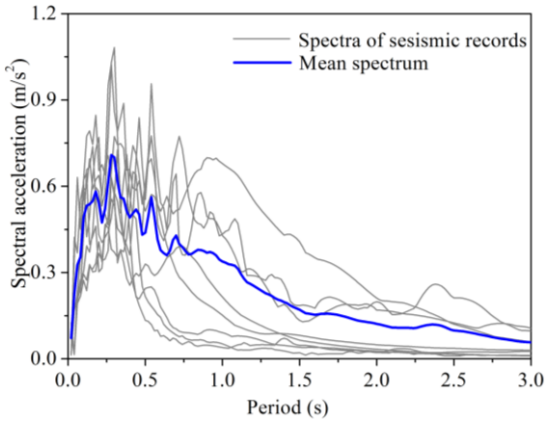

Fig. 5 Acceleration spectra and mean spectrum of selected 8 seismic records

5. Comparisons of the results

5.1 FEHA versus wavelet energy method for a single tower

Based on the Model I, a total of 37 analysis cases are input into ABAQUS to research the maximum peak displacements (between the transverse and longitudinal directions) at the top of the tower and the corresponding incidence angle (i.e., the critical incidence angle) as the incidence angle, θ, varies from 0° to 180° at an increment of 5°. The detailed definition of θ and the input pattern of the seismic wave are discussed in Section 3.3. To present a comparison of the results more clearly, the normalization

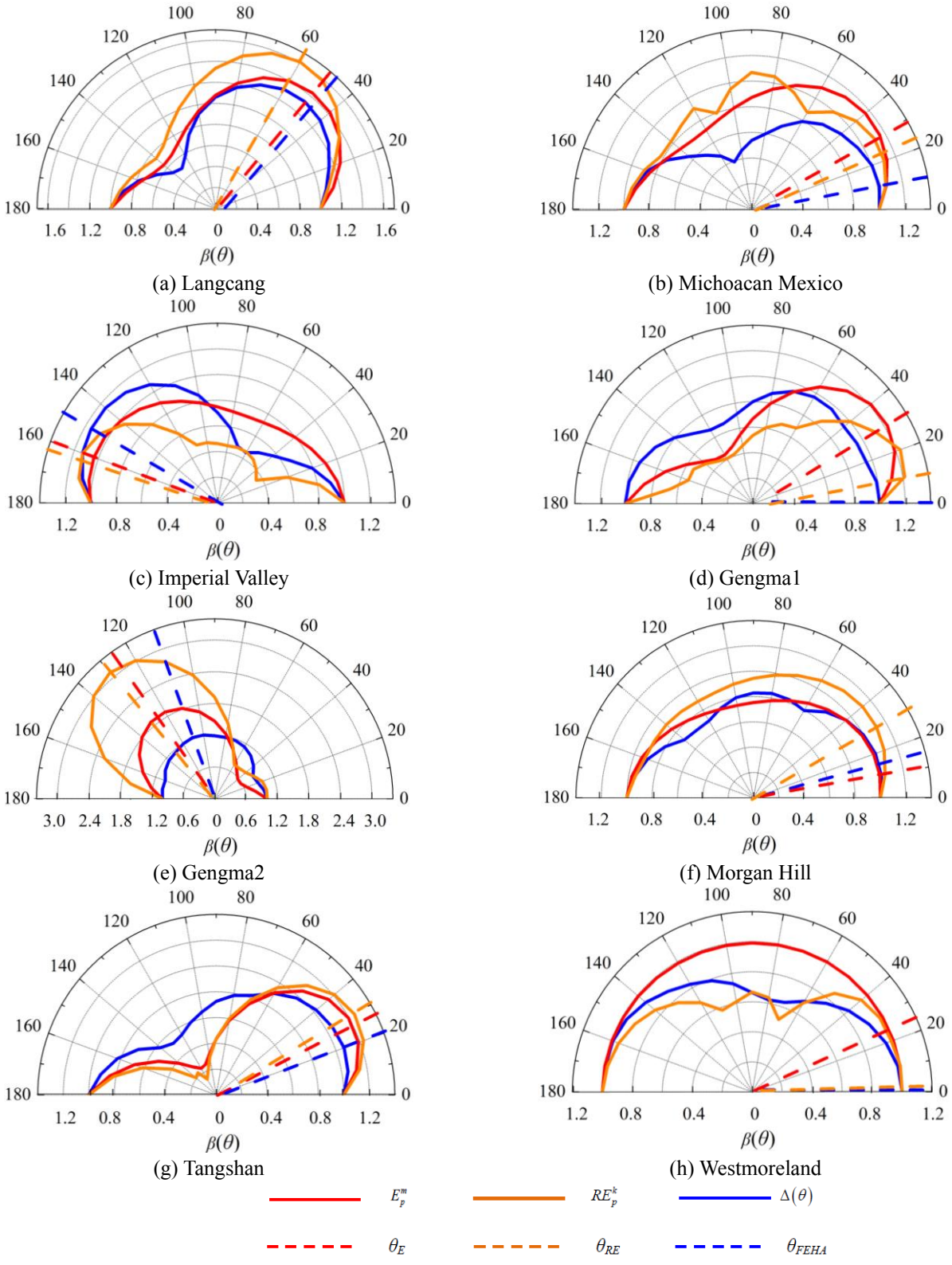

Fig. 6 Normalized curves of the FEHA, effective energy input and effective energy input rate

method is employed by defining $\beta(\theta)$, which is the ratio of the maximum peak displacement response at the top of the tower under different angles θ to that under 0°. Note that the change in the analysis results before and after normalization is consistent, and that $\beta(0°)$ is equal to 1.0 for every ground motion. Furthermore, the incidence angle causing the maximum value of $\beta(\theta)$ is the critical incidence angle, θ_{FEHA}.

Similarly, 37 incidence angles are also investigated with the wavelet energy method. Based on the eigenvalue analysis results, the periods of the first three modes in the longitudinal direction are 0.56, 0.20 and 0.18 s, and the

Table 4 Result comparison: FEHA and wavelet energy method

Seismic record	Num	FEHA	Wavelet energy method				
		θ_{FEHA}/°	θ_E/°	θ_{RE}/°	ΔE_P^M /%	ΔRE_P^K /%	θ_{WEM}/°
Langcang	GM1	50	50	60	2.38	1.53	50
Michoacan Mexico	GM2	10	30	25	1.65	1.57	30
Imperial Valley	GM3	150	160	160	0	0	160
Gengma1	GM4	0	30	15	0.0563	0.1027	15
Gengma2	GM5	110	125	130	0.58	0.84	130
Morgan Hill	GM6	15	10	35	4.06	6.28	35
Tangshan	GM7	20	25	30	0.11	0.26	30
Westmoreland	GM8	0	25	0	0.16	2.05	0

corresponding ratio of the modal participation mass factors is $\Gamma_1^X:\Gamma_2^X:\Gamma_3^X=1:0.45:0.27$. Therefore, the mode combination frequency is calculated to be 1.77 Hz by using Eqs. (5)-(6). According to the steps in Section 3.3 and the frequency of 1.77 Hz, wavelet transformation is subsequently performed to calculate the earthquake total effective energy input E_p^m, and the effective energy input rate, RE_p^k of component, X_θ, under different cases. Note that the identical normalization process is also utilized for E_p^m and RE_p^k, and the critical angle of seismic wave, θ_{WEM}, can be determined by comparing the parameters, E_p^m and RE_p^k.

Fig. 6 compares $\beta(\theta)$ versus different angles for each ground motion obtained from the FEHA (the blue solid line) and wavelet energy method analysis (the red and orange solid lines) of Model I. As showed, the parameters E_p^m and RE_p^k can overall exhibit the similar rules of $\beta(\theta)$ with FEHA, there exists obvious amplitude differences in $\beta(\theta)$, although. This is because the higher-mode effect and the torsional response of the transmission tower are ignored and the displacement response in two horizontal directions is assumed to be independent. Table 4 summarizes the critical incidence angles of different seismic records through FEHA (the blue dotted line) and the wavelet energy method (the red and orange dotted lines). As illustrated, θ_{FEHA} essentially agrees with θ_{WEM} with an error less than 20°, and both angles are identical under GM 1. Interestingly, an obvious difference can be found for the critical incidence angles under different ground motions. Additionally, even if two seismic records are taken from the same earthquake event and only the site classification is different, their critical incidence angles are different. These facts demonstrate that different ground motions and site classifications have a significant influence on the critical incidence angle of earthquakes at single transmission towers.

To quantify the calculation error between the both two methods, λ is defined as follows

$$\lambda=\frac{\beta_{FEHA}(\theta_{FEHA})-\beta_{FEHA}(\theta_{WEM})}{\beta_{FEHA}(\theta_{FEHA})}\times 100\% \tag{11}$$

where, $\beta_{FEHA}(\theta_{FEHA})$ and $\beta_{FEHA}(\theta_{WEM})$ represent the maximum peak displacement response of the transmission tower at θ_{FEHA} and θ_{WEM}, respectively. Fig. 7 plots λ values under different ground motions. As shown, the maximum

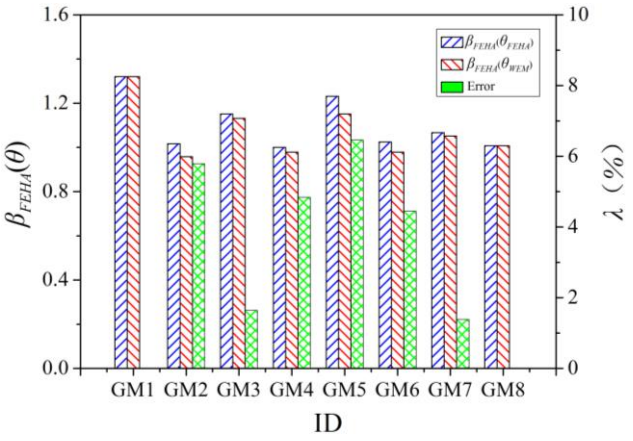

Fig. 7 Evaluation of the underestimation of the maximum value of $\beta_{FEHA}(\theta)$

peak displacement responses at θ_{FEHA} and θ_{WEM} are very close under the eight ground motions studied, and the maximum error value is only 6.5%. This result indicates that wavelet analysis is an attractive and accurate method of predicting the critical angle of seismic incidence of a single transmission tower with high precision.

5.2 FEHA versus wavelet analysis method for a tower-line system

In practice, an electricity transmission system consists of transmission towers and transmission lines. In the prior subsection, the wavelet energy method was verified to be effective for single transmission towers. Therefore, validation work is also executed for Model II, which explicitly considers the spatial coupling effect between transmission towers and transmission lines. Similar to the FEHA for Model I, a total of 37 analysis cases are taken into account, and the incidence angle varies from 0° to 180° with an increment of 5°. Note that only Tower 2 is selected as the study object; thus, its maximum peak displacement response is extracted. Fig. 8 shows $\beta(\theta)$ versus the different angles obtained from the FEHA of Model II.

Subsequently, the value of $\beta(\theta)$ under each incidence angle corresponding to the abovementioned FEHA is also calculated using the wavelet energy method for Model II. As described in Section 2, the periods of the first three modes of the transmission tower-line system in the longitudinal direction are 0.73, 0.63 and 0.21 s, and the

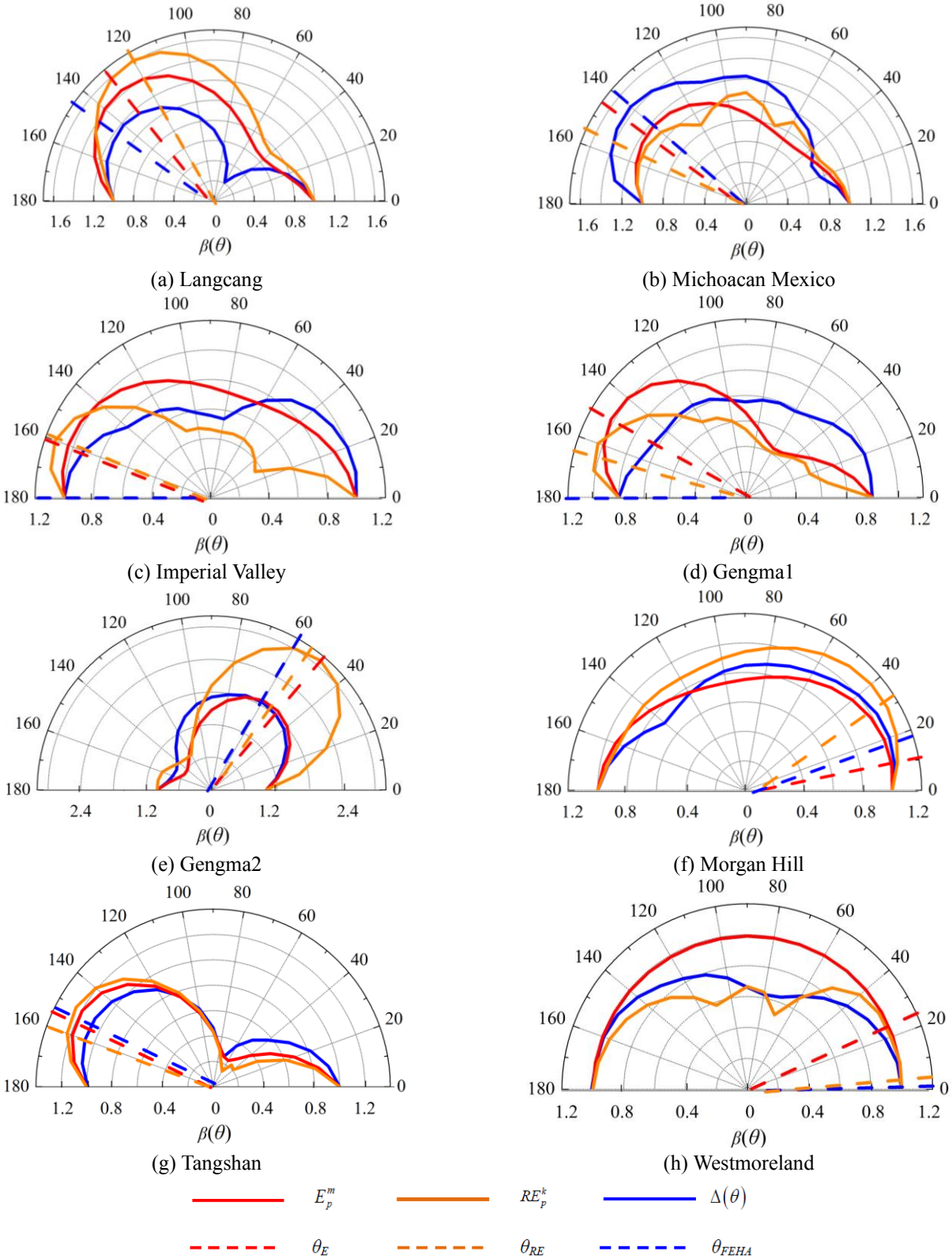

Fig. 8 Normalized curves of the FEHA, effective energy input and effective energy input rate

corresponding ratio of the modal participation mass factors is $\Gamma_1^X:\Gamma_2^X:\Gamma_3^X=1:0.54:0.54$. The mode combination frequency is calculated to be 1.24 Hz and the parameters of E_p^m and RE_p^k are ultimately obtained. For comparison purposes, the $\beta(\theta)$ versus different angles obtained from the wavelet analysis also is plotted in Fig. 8.

Comparatively, the $\beta(\theta)$ values of E_p^m, RE_p^k and the maximum peak displacement response have similar trends with changing earthquake incidence angle. The amplitude differences in $\beta(\theta)$ could still be observed due to model

Table 5 Result comparison: FEHA and wavelet energy method

Seismic record	Num	FEHA	Wavelet energy method				
		θ_{FEHA}/°	θ_E/°	θ_{RE}/°	ΔE_P^M /%	ΔRE_P^K /%	θ_{WEM}/°
Langcang	GM1	145	130	120	2.36	1.57	130
Michoacan Mexico	GM2	140	145	155	1.65	1.57	145
Imperial Valley	GM3	180	160	160	0	0	160
Gengma1	GM4	180	150	165	5.64	10.25	160
Gengma2	GM5	60	55	50	0.58	0.22	55
Morgan Hill	GM6	20	10	35	3.99	6.21	35
Tangshan	GM7	155	155	160	0.11	0.26	160
Westmoreland	GM8	0	25	5	0.16	2.02	5

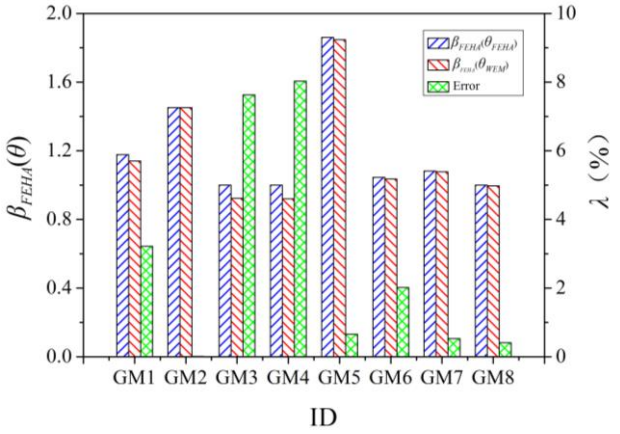

Fig. 9 Evaluation of the underestimation of the maximum value of $\beta_{FEHA}(\theta)$

assumptions and simplifications. The critical incidence angles of different seismic records determined via FEHA and the wavelet energy method are tabulated in Table 5. The critical incidence angles predicted by the wavelet energy method are the same as those obtained from the FEHA, and the maximum error values of the eight seismic records only reach 20°. Without exception, a significant influence of different ground motions and site classifications on the critical incidence angle of earthquakes is observed for transmission tower-line systems. Notably, λ is also applied herein to evaluate the reliability of the wavelet energy method, as shown in Fig. 9. Specifically, the maximum peak displacement responses at θ_{WEM} agree with those at θ_{FEHA}, and the error is within 8.5%. Moreover, the critical incidence angle of the single transmission tower and transmission tower-line system have significant differences for most seismic records, which implies the important influence of the coupling effect between the transmission tower and the transmission line. Overall, for either a single transmission tower or transmission tower-line system, the application of the wavelet energy method is convenient and reliable, which could be used in place of FEHA to avoid time-consuming and costly calculations.

6. Conclusions

This research focuses on investigating the critical seismic incidence of transmission tower-line systems based on the wavelet energy method. Wavelet transformation is performed to obtain the total effective energy input and effective energy input rate to predict the critical incidence angle of the earthquake. To validate this discriminant approach, two computer models, with and without consideration of the interaction between the transmission tower and transmission lines, are developed in ABAQUS. FE analyses are subsequently imposed to generate comparative data for evaluating the effectiveness and accuracy of the wavelet analysis method. Based on the results, the following major conclusions can be drawn:

- The wavelet energy method only requires the natural vibration periods and corresponding participating mass factors of the structure to calculate the two important parameters: the total effective energy input and the effective energy input rate of the ground motions. By comparing these two parameters, the critical incidence angle can be predicted; this approach is more convenient than the conventional time history analysis method.
- A comparison of the results from the wavelet energy method and the time history analysis suggests that the wavelet energy method could predict the critical angle of seismic incidence of both a single transmission tower and a transmission tower-line system with maximum errors less than 10%.
- Compared with the conventional fundamental frequency, the mode combination frequency takes into account the influence of the first three modes by adopting the SRSS rule to more reasonably determine the critical input direction of the ground motions.
- Different ground motions, site classifications and coupling effects between transmission towers and transmission lines have a significant influence on the critical incidence angle of earthquakes for both a single transmission tower and a transmission tower-line system.

In the present study, the critical angle of seismic incidence of transmission tower is investigated by the wavelet energy method. Although it is known that the near-fault ground can result in different dynamic response compared with the far-fault ground motions, the earthquakes types are not distinguished in this investigation. Therefore, research opportunity exists to discuss influences on the critical incidence angle of earthquakes of the near-fault and far-field ground motions. Additionally, both the FE models are developed in ABAQUS without considering

the soil-structure interactions. It is necessary to investigate the influence of the soil-structure interactions on the critical incidence angle of earthquakes in future studies. By incorporating the soil-structure interactions, the wavelet energy method is possible to provide a better prediction of the critical incidence angle of earthquakes.

Acknowledgments

This research was financially supported by the National Natural Science Foundation of China (Awards Nos. 51778347 and 51578325) and the Young Scholars Program of Shandong University (Awards No. 2017WLJH33). Finally yet importantly, the authors wish to thank the anonymous reviewers for their careful evaluations and insightful comments that helped improve the paper.

References

Akehashi, H. and Takewaki, I. (2019), "Optimal viscous damper placement for elastic-plastic MDOF structures under critical double impulse", *Front. Built. Environ.*, **5**. https://doi.org/10.3389/fbuil.2019.00020.

Albermani, F., Kitipornchai, S. and Chan, R.W. (2009), "Failure analysis of transmission towers", *Eng. Fail. Anal*., **16**(6), 1922-1928. https://doi.org/10.1016/j.engfailanal.2008.10.001.

Albermani, F.G.A. and Kitipornchai, S. (2003), "Numerical simulation of structural behaviour of transmission towers", *Thin Wall. Struct.*, **41**(2-3), 167-177. https://doi.org/10.1016/S0263-8231(02)00085-X.

Baranov, S.V. (2007), "Application of the wavelet transform to automatic seismic signal detection", *Izv-Phys. Solid Eart+*, **43**(2), 177-188. https://doi.org/10.1134/S1069351307020085.

Bombale, B.S., Singha, M.K. and Kapuria, S. (2008), "Detection of delamination damage in composite beams and plates using wavelet analysis", *Struct. Eng. Mech.*, **30**(6), 699-712. https://doi.org/10.12989/sem.2008.30.6.699.

Bravo-Imaz, I., Ardakani, H.D., Liu, Z., García-Arribas, A., Arnaiz, A. and Lee, J. (2017), "Motor current signature analysis for gearbox condition monitoring under transient speeds using wavelet analysis and dual-level time synchronous averaging", *Mech. Syst. Signal Pr.*, **94**, 73-84. https://doi.org/10.1016/j.ymssp.2017.02.011.

Cantagallo, C., Camata, G. and Spacone, E. (2012), "The effect of the earthquake incidence angle on seismic demand of reinforced concrete structures", *Proceedings of the 15th World Conference on Earthquake Engineering*, Lisbon, Portugal, September.

Eslamlou, S.D. and Asgarian, B. (2017), "Determining critical areas of transmission towers due to sudden removal of members", *Case Stud. Eng. Fail. Anal.*, **9**, 138-147. https://doi.org/10.1016/j.csefa.2015.09.005.

Fajfar, P. and Vidic, T. (1994), "Consistent inelastic design spectra: hysteretic and input energy", *Earthq. Eng. Struct. D.*, **23**(5), 523-537. https://doi.org/10.1002/eqe.4290230505.

Fujita, K. and Takewaki, I. (2010), "Critical correlation of bi-directional horizontal ground motions", *Eng. Struct*., **32**(1), 261-272. https://doi.org/10.1016/j.engstruct.2009.09.013.

GB 18306-2015 (2015), Seismic Ground Motion Parameters Zonation Map of China, Standardization Administration of China Press, Beijing, China.

GB 2695-82 (1982), Rules of Nomenclature for Transmission Poles and Towers, Electric Power Press, Beijing, China.

GB 50260-2013 (2013), Code for Seismic Design of Electrical Installations, China Architecture & Building Press, Beijing, China.

GB 50545-2010 (2010), Code for Design of 110kV-750kV Overhead Transmission Line, China Architecture & Building Press, Beijing, China.

Ghobarah, A., Aziz, T.S. and El-Attar, M. (1996), "Response of transmission lines to multiple support excitation", *Eng. Struct*., **18**(12), 936-946. https://doi.org/10.1016/S0141-0296(96)00020-X.

Hall, J.F., Holmes, W.T. and Somers, P. (1996), "Northridge earthquake, January 17, 1994", Earthquake Engineering Research Institute, California, USA.

Huang, J.Q., Du, X.L., Jin, L. and Zhao, M. (2016), "Impact of incident angles of P waves on the dynamic responses of long lined tunnels", *Earthq. Eng. Struct. D.*, **45**(15), 2435-2454. https://doi.org/10.1002/eqe.2772.

Kim, H. and Melhem, H. (2004), "Damage detection of structures by wavelet analysis", *Eng. Struct*., **26**(3), 347-362. https://doi.org/10.1016/j.engstruct.2003.10.008.

Kuwamura, H., Iyama, J. and Takeda, T. (1997b), "Energy input rate of earthquake ground motion--matching of displacement theory and energy theory", *J. Struct. Constr. Eng.*, **498**, 37-42.

Kuwamura, H., Takeda, T. and Sato, Y. (1997a), "Energy input rate in earthquake destructiveness-comparison between epicentral and oceanic earthquakes", *J. Struct. Constr. Eng.*, **491**, 29-36.

Lei, Y.H. and Chien, Y.L. (2009), "Seismic analysis of transmission towers under various line configurations", *Struct. Eng. Mech*., **31**(3), 241-264. https://doi.org/10.12989/sem.2009.31.3.241.

Li, H.N., He, X.Y. and Yi, T.H. (2009), "Multi-component seismic response analysis of offshore platform by wavelet energy principle", *Coast. Eng.*, **56**(8), 810-830. https://doi.org/10.1016/j.coastaleng.2009.02.008.

Li, H.N., Shi, W.L., Wang, G.X. and Jia, L.G. (2005), "Simplified models and experimental verification for coupled transmission tower–line system to seismic excitations", *J. Sound Vib*., **286**(3), 569-585. https://doi.org/10.1016/j.jsv.2004.10.009.

Lopez, O.A. and Torres, R. (1997a), "The critical angle of seismic incidence and the maximum structural response", *Earthq. Eng. Struct. D.*, **26**(9), 881-894. https://doi.org/10.1002/(SICI)1096-9845(199709)26:9<881::AID-EQE674>3.0.CO;2-R.

Lopez, O.A., Chopra, A.K. and Hernandez, J.J. (2000a), "Critical response of structures to multicomponent earthquake excitation", *Earthq. Eng. Struct. D.*, **29**(12), 1759-1778. https://doi.org/10.1002/1096-9845(200012)29:12<1759::AID-EQE984>3.0.CO;2-K.

Magliulo, G., Maddaloni, G. and Petrone, C. (2014), "Influence of earthquake direction on the seismic response of irregular plan RC frame buildings", *Earthq. Eng. Eng. Vib.*, **13**(2), 243-256. https://doi.org/10.1007/s11803-014-0227-z.

Menun, C. and Der Kiureghian, A. (1998), "A replacement for the 30%, 40%, and SRSS rules for multicomponent seismic analysis", *Earthq. Spectra*, **14**(1), 153-163. https://doi.org/10.1193/1.1585993.

Montanari, L., Basu, B., Spagnoli, A. and Broderick, B.M. (2015), "A padding method to reduce edge effects for enhanced damage identification using wavelet analysis", *Mech. Syst. Signal Pr*., **52**, 264-277. https://doi.org/10.1016/j.ymssp.2014.06.014.

Rigato, A.B. and Medina, R.A. (2007), "Influence of angle of incidence on seismic demands for inelastic single-storey structures subjected to bi-directional ground motions", *Eng. Struct*., **29**(10), 2593-2601. https://doi.org/10.1016/j.engstruct.2007.01.008.

Rosenblueth, E. (1951), "A basis for aseismic design", Ph.D. Dissertation, Univ. of Illinois, Urbana, IL.

Roy, A., Santra, A. and Roy, R. (2018), "Estimating seismic response under bi-directional shaking per uni-directional

analysis: Identification of preferred angle of incidence", *Soil Dyn. Earthq. Eng*., **106**, 163-181. https://doi.org/10.1016/j.soildyn.2017.12.022.

Shinozuka, M. (1995), "The Hanshin-Awaji earthquake of January 17, 1995 Performance of life lines", Report NCEER-95-0015, NCEER.

Smeby, W. and Der Kiureghian, A. (1985), "Modal combination rules for multicomponent earthquake excitation", *Earthq. Eng. Struct. D.*, **13**(1), 1-12. https://doi.org/10.1002/eqe.4290130103.

Taha, M.R., Noureldin, A., Lucero, J.L. and Baca, T.J. (2006), "Wavelet transform for structural health monitoring: a compendium of uses and features", *Struct. Health Monit.*, **5**(3), 267-295. https://doi.org/10.1177/1475921706067741.

Takewaki, I. (2013), *Critical Excitation Methods In Earthquake Engineering*, Butterworth-Heinemann, London, England

Taniguchi, R., Kojima, K. and Takewaki, I. (2016), "Critical response of 2DOF elastic-plastic building structures under double impulse as substitute of near-fault ground motion", *Front. Built. Environ.*, **2**, 2. https://doi.org/10.3389/fbuil.2016.00002.

Tian, L., Fu, Z., Pan, H., Ma, R. and Liu, Y. (2019c), "Experimental and numerical study on the collapse failure of long-span transmission tower-line systems subjected to extremely severe earthquakes", *Earthq. Struct*., **16**(5), 513-522. https://doi.org/10.12989/eas.2019.16.5.513.

Tian, L., Pan, H. and Ma, R. (2019a), "Probabilistic seismic demand model and fragility analysis of transmission tower subjected to near-field ground motions", *J. Constr. Steel Res*., **156**, 266-275. https://doi.org/10.1016/j.jcsr.2019.02.011.

Tian, L., Pan, H., Ma, R. and Qiu, C. (2017), "Collapse simulations of a long span transmission tower-line system subjected to near-fault ground motions", *Earthq. Struct*., **13**(2), 211-220. : https://doi.org/10.12989/eas.2017.13.2.211.

Tian, L., Rong, K., Bi, K. and Zhang, P. (2019b), "A bidirectional pounding tuned mass damper and its application to transmission tower-line systems under seismic excitations", *Int. J. Struct. Stab. Dyn.*, **19**(6), 1950056. https://doi.org/10.1142/S0219455419500561.

Tian, L., Yi, S. and Qu, B. (2018), "Orienting ground motion inputs to achieve maximum seismic displacement demands on electricity transmission towers in near-fault regions", *J. Struct. Eng*., **144**(4), 04018017. https://doi.org/10.1061/(ASCE)ST.1943-541X.0002000.

Torbol, M. and Shinozuka, M. (2012), "Effect of the angle of seismic incidence on the fragility curves of bridges", *Earthq. Eng. Struct. D.*, ***41***(14), 2111-2124. https://doi.org/10.1002/eqe.2197.

Uang, C.M. and Bertero, V.V. (1990), "Evaluation of seismic energy in structures", *Earthq. Eng. Struct. D.*, **19**(1), 77-90. https://doi.org/10.1002/eqe.4290190108.

Wilson, E.L. and Button, M.R. (1982), "Three-dimensional dynamic analysis for multi-component earthquake spectra", *Earthq. Eng. Struct. D.*, **10**(3), 471-476. https://doi.org/10.1002/eqe.4290100309.

Wimarshana, B., Wu, N. and Wu, C. (2017), "Crack identification with parametric optimization of entropy & wavelet transformation", *Struct. Monit. Maint.*, **4**(1), 33-52. https://doi.org/10.12989/smm.2017.4.1.033.

Wu, G., Zhai, C., Li, S. and Xie, L. (2014), "Effects of near-fault ground motions and equivalent pulses on large crossing transmission tower-line system", *Eng. Struct.*, **77**, 161-169. https://doi.org/10.1016/j.engstruct.2014.08.013.

Xie, L.L. and Zhai, C.H. (2003), "Study on the severest real ground motion for seismic design and analysis", *Acta Seismologica Sinica*, **25**, 250-261. https://doi.org/10.1007/s11589-003-0030-9.

Yamamoto, K., Fujita, K. and Takewaki, I. (2011), "Instantaneous earthquake input energy and sensitivity in base-isolated building", *Struct. Des. Tall Spec.*, **20**(6), 631-648. https://doi.org/10.1002/tal.539.

Yuntian, F., Mingrui, L. and Chunzhe, L. (1991), "Elastic earthquake response analysis for complex structures", *Earthq. Eng. Eng. Vib.*, **11**(4), 77-86.

Zhang, P., Song, G., Li, H.N. and Lin, Y.X. (2012), "Seismic control of power transmission tower using pounding TMD", *J. Eng. Mech*., **139**(10), 1395-1406. https://doi.org/10.1061/(ASCE)EM.1943-7889.0000576.

Zhao, B. and Taucer, F. (2010), "Performance of infrastructure during the May 12, 2008 Wenchuan earthquake in China", *J. Earthqu. Eng*., **14**(4), 578-600. https://doi.org/10.1080/13632460903274053.

Zheng, H.D., Fan, J. and Long, X.H. (2017), "Analysis of the seismic collapse of a high-rise power transmission tower structure", *J. Constr. Steel Res*., **134**, 180-193. https://doi.org/10.1016/j.jcsr.2017.03.005.

AT